BIOCHEMISTRY
including biophysical chemistry & molecular biology

Article

pubs.acs.org/biochemistry

L105K Mutant of Proteorhodopsin

Tushar Kanti Maiti, Keisuke Yamada, Keiichi Inoue, and Hideki Kandori*

Department of Frontier Materials, Nagoya Institute of Technology, Showa-ku, Nagoya 466-8555, Japan

Supporting Information

ABSTRACT: Proteorhodopsin (PR) is a light-driven proton pump found in marine bacteria. Thousands of PRs are classified into blue-absorbing (λ_{max} ~ 490 nm) and green-absorbing (λ_{max} ~ 525 nm) PR, and the color determinant is known to be at position 105, where blue-absorbing and green-absorbing PR possess Gln and Leu, respectively. Position 105 is in contact with the retinal chromophore in the hydrophobic region of the cytoplasmic side. In this paper, we have introduced a positively charged lysine group at position 105, which is the first report of the introduction of a positively charged group into the hydrophobic cytoplasmic domain in microbial rhodopsins. The L105K mutant PR shows an ~21 nm red shift (λ_{max} ~ 549 nm) at pH 7.0, and the pK_a of the counterion (7.2) does not change significantly compared to that of wild-type PR (6.8). The analysis of thermal stability shows that the mutation causes some destabilization of structure, but the mutant is more stable toward hydroxylamine reaction than the wild type. The flash photolysis measurement at pH 9.0 shows that the decay of the M intermediate of L105K is ~3 times slower than that of the wild type. The slow M decay possibly originates from the perturbation of the proton donor (Glu108) and the retinal Schiff base due to positioning of a positively charged lysine group in the proton transfer pathway. The perturbation of proton transport is also observed when we measure light-induced proton pumping. The rate of proton transport in L105K mutant is 6 times slower than that of the wild type, which corroborates our flash photolysis result.

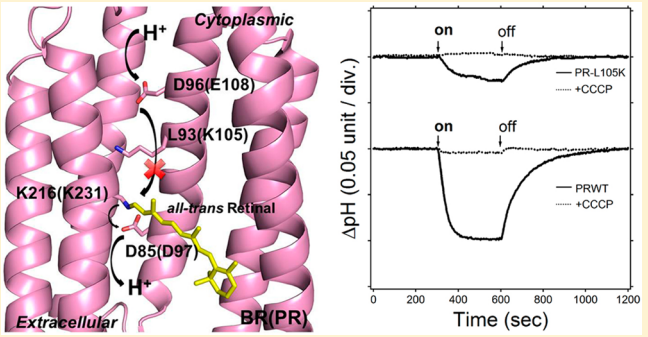

Retinal proteins are widely distributed in nature from archaea to humans. Retinal plays a crucial role in vision in the animal kingdom, whereas its function in ion transport, as a phototactic sensor, is also well understood in microbial rhodopsins, which are found in extreme haloarchaea, bacteria, and eukaryotic microorganisms.[1] The two families, visual and microbial rhodopsins, share an identical structural motif, characterized by seven transmembrane helices and a retinal chromophore covalently bound to an ε-amino group of a conserved lysine in the seventh helix via a protonated Schiff base (PSB) linkage.[2,3] However, they do not share any significant similarities in their sequence possibly because of their different evolutionary origins. In a methanol solution, a protonated retinylidene Schiff base exhibits a λ_{max} at 440 nm.[4,5] The protein microenvironment shifts the λ_{max} to longer wavelengths, e.g., to 487 nm in sensory rhodopsin II, 568 nm in bacteriorhodopsin, and 578 nm in halorhodopsin from *Halobacterium salinarum*.[6] The retinal binding proteins can thus tune the absorption of these chromophores by specific interactions to an exact maximum. The color tuning mechanism is one of the important aspects of the rhodopsin field, because the color of a common molecule, either 11-*cis*-retinal (visual rhodopsin) or all-*trans*-retinal (microbial rhodopsin) Schiff base, is determined by the surrounding amino acids of the protein.[7−11] Even though it has been investigated for several decades, the molecular mechanism underlying it is still not clear. It is likely that color tuning is determined by various interactions between the retinal chromophore and protein, such as the electrostatic effect of charged groups, dipole interactions with polar amino acids, aromatic amino acids, hydrogen bonding interactions, and steric effects.[1,7−11]

The retinal−protein interactions in rhodopsins have been experimentally verified by site-directed mutagenesis. Many mutations were introduced into bacteriorhodopsin (BR), a microbial rhodopsin that acts as a light-driven proton pump. For example, in the case of the D85N mutant of BR, the color changes from purple (λ_{max} ~ 560 nm) to blue (λ_{max} ~ 600 nm).[12] The reason for the spectral red shift is that the negatively charged counterion (Asp85) is neutralized. On the other hand, the color changes from purple (~560 nm) to reddish (~530 nm) for the L93A and L93T mutants, where specific chromophore−protein interaction is modified.[13] Thus, electrostatic and steric effects at Asp85 and Leu93, respectively, contribute significantly to the color tuning in BR. Similarly extensive mutational studies have also been performed in the retinal binding pocket, where hydrophobic residues like Val49, Ala53, Trp82, and Trp182 alter the retinal−protein interactions, leading to the modification of the photocycle and absorption maxima.

Received: December 23, 2011
Revised: March 25, 2012
Published: March 29, 2012

 © 2012 American Chemical Society

Over the past several years, a new type of retinal protein named proteorhodopsin (PR) derived from the bacterial domain has been discovered through genomic analyses of naturally occurring marine γ-proteobacteria and was expressed in *Escherichia coli*.[14] The γ-proteobacteria having PRs are widely distributed in the Pacific Ocean, the Red Sea, the Japan Sea, and other similar environments.[15] This suggests the possibility of a previously unrecognized phototrophic pathway that may influence the flux of carbon and energy in the ocean's photic zone worldwide. In fact, we have recently succeeded in directly measuring proton-pump activity of PR in native flavobacterial cells.[16] The amino acid sequence of PR shows a high degree of similarity to the sequences of the microbial rhodopsins,[14,17] and it can be classified into blue-absorbing ($\lambda_{max} \sim 490$ nm) and green-absorbing ($\lambda_{max} \sim 525$ nm) PR according to their absorption maxima. The absorption maxima of the pigments are tuned to the depth at which the specific bacteria live. Those living in the upper layers of the ocean absorb at longer wavelengths, whereas those that exist in deeper layers absorb at shorter wavelengths, in keeping with the available light able to penetrate the water.[17−19] Light absorption by PR triggers a series of conformational changes associated with the chromophore and the protein environment and results in the translocation of a proton from the cytoplasmic side to the extracellular surface.[14,16,17,20] The electrochemical gradient generated by this process is used to drive ATP synthesis for fueling metabolic processes within the cell.[21]

Previous studies showed that one of the determinants of color tuning of PR is at position 105, where blue-absorbing or green-absorbing PR possesses Gln or Leu, respectively.[18,19] Man et al. have shown that the switch of GPR into BPR is possible because of the interchange of Leu105 with Gln, and vice versa.[19] The corresponding amino acid in BR is Leu93, which is in direct contact with the 13-methyl group of the retinal chromophore. Although the structure of PR has not been determined, the L/Q switch for color tuning presumably is caused by the direct contact with the retinal chromophore.[22] On the other hand, the color mechanism has not been well understood. The interhelical cavity of microbial rhopdopsins is divided by the Schiff base into the extracellular and cytoplasmic "half-channels" that together describe the trajectory of transported protons.[23] The extracellular half-channel contains numerous charged or hydrogen bonding residues as well as water molecules, whereas the cytoplasmic region is mostly hydrophobic. The L/Q switch of PR is located in the cytoplasmic region, where the L-to-Q mutation in GPR[19] and L-to-T or L-to-A mutation in BR[13] cause a spectral blue shift. Does this mean that polar groups at this position yield a spectral blue shift? In this study, we attempted to introduce a positively charged lysine group at this position of PR, which might cause a further blue shift. It should be noted that no charges have been introduced into the hydrophobic cytoplasmic domain of microbial rhodopsins. BR possesses Asp96 in the cytoplasmic domain, whereas it is well-known that Asp96 has no negative charge (aspartic acid is protonated in the unphotolyzed state). Here we successfully expressed the L105K mutant PR, which exhibited a spectral red shift, not a blue shift. Various molecular properties are compared between L105K and the wild type.

MATERIALS AND METHODS

Expression and Purification of the L105K Mutant of GPR. The expression plasmids were constructed as described previously.[24,25] To avoid oxidation of cysteine residues, a triple-cysteine mutant (C107S/C156S/C175S) was used as a template for the mutagenesis.[26,27] We regarded this protein as the wild type and introduced additional mutations. Mutations were performed using the QuickChange site-directed mutagenesis kit (Stratagene) according to the manufacturer's protocol. Proteorhodopsin having six histidines at the C-terminus was expressed in *E. coli*. The protein was solubilized with 0.1% *n*-dodecyl β-D-maltoside (DDM) and purified via Ni-NTA column chromatography.[24,28]

UV−Visible Spectroscopy. Absorption spectra of detergent-solubilized PR (0.1% DDM, 150 mM NaCl, 10 mM citric acid monohydrate, MES, MOPS, HEPES, CHES, and CAPS) were recorded using a Shimadzu UV-2400PC UV−visible spectrophotometer at 25 °C.[24] The initial pH was 4−5, from which the pH was increased to 10 by the addition of NaOH. The absorption spectra were measured at every 0.5 pH unit. Once the pH of the solution reached 10, it was again lowered to 4.0 by addition of HCl. We have confirmed that absorption spectra at the same pH produced by addition of either NaOH or HCl were identical, indicating that pH titration was reversible between pH 4 and 10 for all proteins. The absorption maxima were plotted as a function of pH, and the data were fit with the Henderson−Hasselbalch equation to determine the pK_a of the counterion.

Thermal Stability of PR-WT and the L105K Mutant. We measured the thermal stability of PR-WT and the L105K mutant by incubating the 0.25 OD sample at 75 °C.[24] The progress of the thermal reaction was monitored by measuring the absorbance change at absorption maxima with time. For each measurement, the reaction was quenched by incubating the sample on ice and the sample was spun for 1 min at 7000 rpm and 4 °C to remove the denatured protein.

Hydroxylamine Reaction. The reactions of PR-WT and the L105K mutant with hydroxylamine were conducted at pH 6.8 and 7.2, respectively. The reaction was initiated by addition of hydroxylamine at a final concentration of 50 mM. The absorption spectra were measured at different time intervals. The temperature of the reaction was maintained 25 °C throughout the experiment.

Pulsed Laser Flash Photolysis. Pulsed laser photolysis was conducted using laser pulses from a Nd^{3+}:YAG laser (532 nm).[29] The samples were dialyzed against 50 mM Tris-HCl buffer (pH 9.0) with 0.1% DDM and 150 mM NaCl. Flash-induced absorption changes were acquired with a 1 ms interval using a commercial flash photolysis system. Excitation of the sample was accomplished using 532 nm nanosecond laser pulses from a Nd^{3+}:YAG laser apparatus. Subsequent spectral changes upon laser excitation were collected consecutively. For signal-to-noise improvement, 20 photoreactions were averaged for each sample solution. The absorbance at λ_{max} (534 nm) was 0.45 before and after the experiment, indicating there is no laser-induced damage to the sample. The temperature of each sample was kept at 25 °C.

Light-Induced Proton Transport. The proton transport activity of each protein was measured by monitoring pH changes in the *E. coli* suspension in water containing 50 mM $MgCl_2$ and 150 mM NaCl by a glass electrode.[25] The pH values of PR-WT and the L105K mutant were adjusted to 6.8 and 7.2, respectively, according to their pK_a of the counterion (Asp97). The samples were illuminated at >450 nm through a glass filter (AGC Techno Glass Y-52), and the pH changes were monitored (F-55 pH meter, Horiba). The light source was a

1 kW tungsten−halogen projector lamp (Master HILUX-HR, Rikagaku). The samples were again illuminated after addition of carbonyl cyanide *m*-chlorophenylhydrazone (CCCP) to a final concentration of 10 μM. The amount of protein in the *E. coli* suspension was estimated by measuring absorption spectra after solubilization of the protein with 1% DDM, 100 μg/mL lysozyme, and 100 μg/mL DNase I for the calculation of initial velocity.

RESULTS

Spectral Comparison of the Wild Type and L105K Mutant. The absorption spectra of wild-type PR and its L105K mutant protein were measured at pH 7.0. Figure 1 shows the

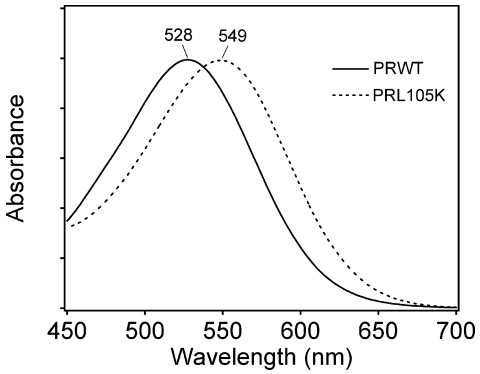

Figure 1. Absorption spectra of wild-type (—) and L105K mutant (···) PRs at pH 7.0. The spectra were measured for the detergent-solubilized sample at 20 °C. The λ_{max} is located at 528 nm (wild type) and 549 nm (L105K).

absorption spectra of the wild type and L105K mutant. The λ_{max} of the L105K mutant is 21 nm red-shifted compared to that of wild-type PR. It is, however, noted that the counterion of the Schiff base is PR Asp97, and the pK_a values for wild-type PR and its L105K mutants are ~6.8 ± 0.15 and 7.2 ± 0.10, respectively. This indicates that both protonated and deprotonated forms are present at neutral pH. Figure 2a shows pH titration curves of the wild type (dotted line with triangles) and L105K mutant (line with circles). The pH titration data were fit with the Henderson−Hasselbalch

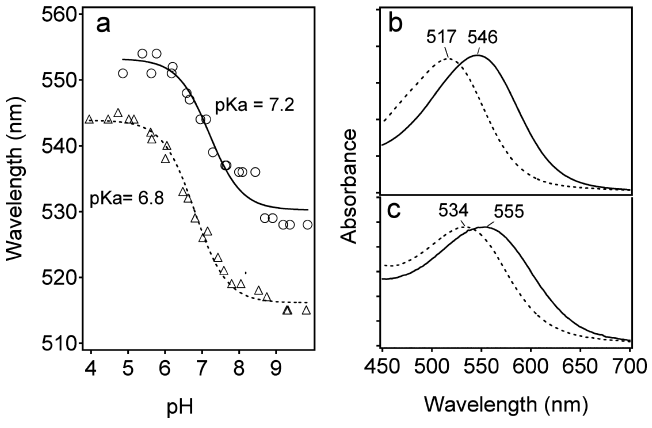

Figure 2. (a) pH titration of wild-type (△) and L105K mutant (○) PRs. (b) Absorption spectra of wild-type PR at pH 5.0 (—) and pH 10.0 (···). (c) Absorption spectra of the L105K mutant at pH 5.0 (—) and pH 10.0 (···).

equation (n = 1). Panels b and c of Figure 2 show absorption spectra of the wild type and L105K mutant at pH 5 (solid curves) and pH 10 (dotted curves), respectively. Because the absorption spectra of both the wild type and its L105K mutant at various pH values exhibit a single isosbestic point (Figure S1 of the Supporting Information), only two forms, with protonated and deprotonated Asp97, are in equilibrium.

It has been shown previously that the various interactions between the chromophore and protein control the color tuning in rhodopsins, and it is also experimentally established that most of the effect is local. As position 105 is just one helical turn below the proton donor position (Glu108) in the same helix, there is a possibility of charge interaction between Lys105 and Glu108. To verify this possibility, we have compared the absorbance maxima of the E108Q mutant and the L105K/E108Q double mutant at pH 7.0. The absorption maxima of the double mutant and the E108Q mutant are 552 and 532 nm, respectively. The double mutant also shows a 20 nm red shift compared to that of E108Q (Figure S2 of the Supporting Information). The pH titration of E108Q shows that the pK_a value of the counterion is not changed significantly (6.7), whereas the double mutant shows a significant deviation in its pK_a value compared to that of the wild type (7.9) (Figure S3 of the Supporting Information). Thus, formation of the salt bridge between Lys105 and Glu108 is unlikely for the L105K mutant.

Thermal Stability and Hydroxylamine Reaction. It has to be noted that mutations often destabilize protein structure, so that the weakened chromophore−protein interaction results in a color change. To verify this possibility, we have tested the protein stability by keeping the sample at 75 °C for 45 min at pH 6.8 and 7.2 for the wild type and L105K mutant, respectively, where the pigment gradually thermally decomposes. Figure 3 shows the decrease in the amount of pigment

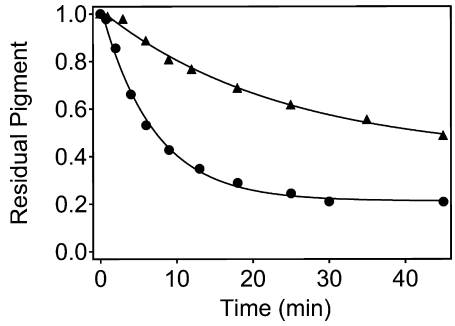

Figure 3. Protein thermal stability of wild-type (▲) and L105K (●) PRs. The samples were kept at 75 °C.

with time in wild-type PR and the L105K mutant. The plots are fit with a single-exponential rate constant, and the half-lives of thermal decay of wild-type PR and the L105K mutant are 23.7 and 6.9 min, respectively. The thermal decomposition of the L105K mutant is almost 3 times faster than that of wild-type PR.

The progress curves of hydroxylamine reaction of wild-type PR at pH 6.8 and the L105K mutant at pH 7.2 are presented in Figure 4. The data were fit with a single-exponential decay rate constant for the wild type and L105K mutant with half-lives of 5.3 and 17.5 min, respectively. It is observed that the rate of hydroxylamine reaction in the L105K mutant is almost 3 times slower than that of wild-type PR.

dx.doi.org/10.1021/bi201916a | *Biochemistry* 2012, 51, 3198−3204

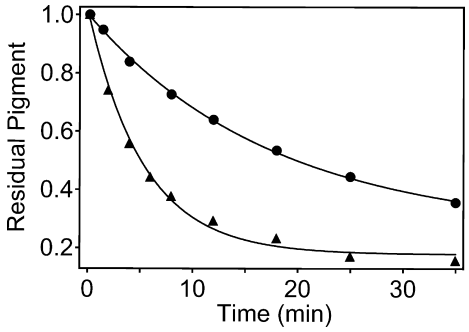

Figure 4. Hydroxylamine reaction of wild-type (▲) and L105K (●) PRs. The hydrolysis reactions were conducted in the presence of 50 mM hydroxylamine at pH 6.8 and 7.2 for the wild type and L105K mutant, respectively.

Pulsed Laser Flash Photolysis. At high pH values, the PR protein is known to function as a proton pump and transfer the proton from the cytoplasmic side to the extracellular side of the membrane. The proton translocation is associated with the light-induced structural change of the chromophore. The photocycle of PR shares a high degree of similarity with the photocycle of BR and exhibits K, L M, N, and O intermediates. From the sequence analysis, it has been observed that the green-absorbing PR and blue-absorbing PR share a high degree of amino acid identity, and it is well-known that the L105Q replacement converts GPR to BPR and vice versa. Figure 5a shows the transient absorption change at the three characteristic wavelengths after flash illumination in wild-type PR at pH 9.0. The negative absorption change at 512 nm originates from depletion of the initial state. The positive absorption change at 590 nm indicates the accumulation of the O intermediate. Any absorption change at 406 nm would indicate the formation of an M-like intermediate with a deprotonated retinal Schiff base. The M-like intermediate is observed only at higher pH values, and it is not seen at low pH values. Global fitting analysis of PR-WT data shows the presence of K, L, M, and O intermediates. Figure 5b shows the corresponding results for L105K PR, where the same intermediates are observed with modified kinetics. The time constants obtained by global fitting for the wild type and L105K are given in Table S1 of the Supporting Information. We also measured the kinetics of E108Q and L105K/E108Q, which exhibit a much slower photocycle because of the lack of the O intermediate (Figure S4 of the Supporting Information). Kinetic parameters of E108Q and L105K/E108Q from global fitting are listed in Table S2 of the Supporting Information.

Light-Induced Proton Transport. Light-driven proton transport was assessed for *E. coli* cells of wild-type and L105K PR by monitoring the pH change with a glass electrode. The bottom panel of Figure 6 shows the light-induced pH changes of wild-type PR at pH 6.8. In case of the wild type at pH 6.8 (the pK_a of the counterion is 6.8), illumination caused a net acidification of the medium (solid curve), indicating the protons are pumped out of the *E. coli* cell. Addition of 10 μM CCCP almost abolishes the observed light-induced pH change (dotted line). Similarly, illumination of *E. coli* cells having L105K PR at pH 7.2 (counterion pK_a = 7.2) (top panel) caused net acidification of the medium (solid line in the top panel), indicating that the protons are pumped out of the *E. coli* cell. Addition of 10 μM CCCP abolished the observed light-induced pH change (dotted line in the top panel). The

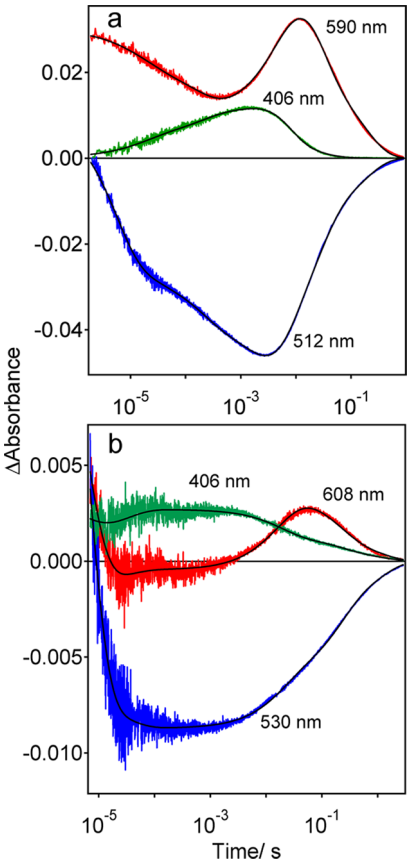

Figure 5. Kinetics of the light-induced absorption change of wild-type (a) and L105K mutant (b) PRs in 0.1% DDM-solubilized samples at pH 9.0 and room temperature. The green trace (406 nm) is for the M intermediate; the red trace is for the O intermediate (590 nm for the wild type and 608 nm for the L105K mutant), and the blue trace is for PR recovery (512 nm for the wild type and 530 nm for the L105K mutant).

pumping data (*y*-axis in Figure 6) are normalized for differences in expression levels of wild-type and L105K PR, using their

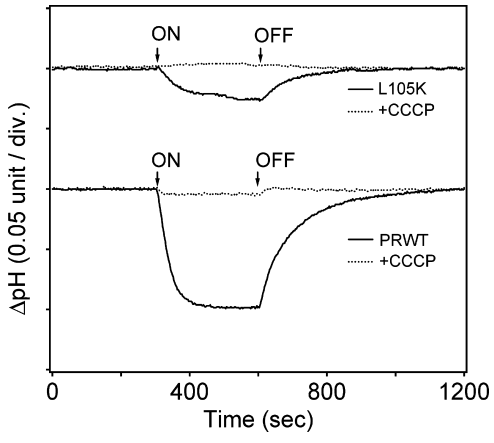

Figure 6. Light-driven proton pumping activity of the *E. coli* sample containing wild-type (bottom) and L105K mutant (top) PR. ON and OFF indicate the onset and offset of illumination (with yellow light, >450 nm) and a negative signal corresponding to a decrease in pH (outward proton pump), respectively. The pH values of the wild type and L105K mutant are 6.8 and 7.2, respectively. The dotted lines represent identical measurements in the presence of 10 μM CCCP.

dx.doi.org/10.1021/bi201916a | *Biochemistry* 2012, 51, 3198−3204

visible absorption spectra after the pumping measurements. The initial slopes of both wild-type and L105K mutant PR were determined. The ratio between wild-type PR and the L105K mutant is 3:1. Thus, the proton pumping activity is substantially reduced because of the L105K mutation.

DISCUSSION

In PR, position 105 (L93 in BR) is very important for color regulation.[19] The amino acid residue in that position in all microbial rhodopsins directly interacts with the 13-methyl group of the retinal chromophore. While the structure of PR has not been determined by X-ray crystallography, solid-state NMR has provided important structural characteristics of PR.[30−34] In addition, the three-dimensional structure of PR has been recently reported by solution NMR,[35] which also confirms the contact between L105 and the 13-methyl group of the retinal chromophore. Therefore, mutation of this position undoubtedly modifies this specific interaction leading to color regulation as well as functional properties. Structural studies of microbial rhodopsins reveal that this position is surrounded by a highly hydrophobic environment. The studies of mutations at this position performed so far included a replacement of hydrophobic residues like Ala. We have introduced a positively charged group lysine for the first time and shown that the protein can be expressed, though the yield was approximately half of that of wild-type PR.

Introduction of a lysine residue leads to a 21 nm red shift compared to that of the wild-type protein at pH 7.0. This red shift (9−17 nm) is also observed in both the protonated and the deprotonated state (Figure 1). One of the key arguments about the red shift is that protonated Schiff base−counterion interaction is weakened by altering the pK_a of the counterion. Previously, we have found color tuning in the case of the PR A178R mutation in the EF loop that is almost 25−30 Å away from the counterion.[24,25] Later we replaced Ala178 with 19 amino acids and came to the conclusion that the size of the amino acid is important in color regulation of this PR mutant.[36] There is a linear correlation between pK_a and λ_{max}. The mechanism of such a distance effect has not yet been determined, but almost all color changing mutations are associated with the alteration of the counterion pK_a, proving that the mutation changes the interaction of the protonated Schiff base and counterion (D97 and D227). As there is no significant change in the pK_a of the counterion in the L105K mutant (0.4 unit increase) (Figure 2a), there is a minimal effect on the counterion because of this mutation.

Position 105 is just one turn below Glu108 in helix C. Thus, one can argue a charge interaction between positively charged lysine and negatively charged glutamate exists. To verify this possibility, we have measured the absorption spectra of E108Q and the L105K/E108Q double mutant. We have seen a similar 20 nm red shift between E108Q and the double mutant (Figure S1 of the Supporting Information). This observation suggests that Lys does not form a salt bridge to the glutamate residue in the unphotolyzed state.

The red shift of the L105K mutant can also be explained considering the opsin shift. The opsin shift is the difference in the absorption of RSB in solution and in a protein environment. In wild-type PR, the opsin shift (OS) is ∼3500 cm^{-1}, whereas for the L105K mutant, the OS is ∼4250 cm^{-1}. A larger opsin shift indicates the chromophore is tightly interacting with protein residues, which reduces the size of the $\pi-\pi^*$ gap in the ground state.

The thermal reaction shows that the mutant is almost 3 times less stable than the wild-type protein, whereas the hydroxylamine reaction shows the mutant is 3 times more stable toward the hydroxylamine reaction. Khorana and his co-workers have reported previously the slower rate of the hydroxylamine reaction in the case of bacteriorhodopsin D85N, D85A, and D212E mutants where mutation causes the red shift of λ_{max}.[37] In the L105K mutant, a similar effect is also observed. There is a possibility of weakening of retinal−protein interaction because of the introduction of a long chain flexible lysine residue at position 105, which is manifested in the lower stability of this mutant. On the other hand, the hydroxylamine reaction shows that the L105K mutant is almost 3 times more stable than wild-type PR (Figure 4). The slow rate of reaction with hydroxyl amine may be explained again in terms of opsin shift. A larger opsin shift in the L105K mutant protein compared to the wild type suggests more chromophore interaction, and hence, the nucleophilic reaction (water or hydroxylamine) will be perturbed in the L105K mutant.

We have checked the photocycle of mutant proteins and compared it with that of the wild type. In the M intermediate, protonation and deprotonation of the retinal Schiff base are necessary for the transfer of the proton from the cytoplasmic side to the extracellular side. The global analysis of wild-type PR data shows that the formation of the M intermediate can be fit as the sum of three exponentials with time constants of 20 μs, 0.18 ms, and 2.1 ms, and we have assigned these intermediates as K-L(M), K-L(M), and L-M, respectively. On the other hand, the transition of the M-O intermediate has a time constant of 5.6 ms, and the decay of O to PR has shown a biphasic decay with time constants of 26 and 180 ms (Table S1 of the Supporting Information). In the L105K mutant, we have detected M (K-M) formation and M (M-O) decay that have time constants of 30 μs and 18 ms, respectively, whereas the decay of O-PR shows a biphasic decay with time constants of 203 and 1130 ms (Table S1 of the Supporting Information). From the flash photolysis analysis, it is clear that the decays of the M-intermediate and O-intermediates are perturbed because of the L105K mutation. The decay of M (M-O) is almost 3 times slower and the decay of O intermediates also 6−8 times slower in the L105K mutant than in the wild-type protein. On the other hand, the formation of the M intermediate, which is associated with the transfer of a proton from PSB to D97, is rather faster in L105K. Consequently, the M state is more stable in L105K. Because a positive charge is introduced near the Schiff base group, Coulombic perturbation possibly causes a decrease in the Schiff base pK_a during the photocycle, leading to an increase in the rate of Schiff base deprotonation and a decrease in the rate of Schiff base reprotonation.

The E108Q mutant and double mutant do not show an O intermediate, and M intermediates directly return to PR (M-PR) (Figure S2 of the Supporting Information). Global fitting analysis shows that the decay of M to PR in both E108Q and double mutants is very slow due to the lack of a proton donor (Glu108), and both E108Q and the double mutant show similar rate constants. The important observation in these mutants is that the formation of the M intermediate in the double mutant is faster than that of E108Q (Table S1 of the Supporting Information), which is also consistent with the results for L105K.

In summary, from the observations described above, we conclude that the positioning of the lysine group stabilizes the deprotonation state of the Schiff base presumably by

Couloumbic perturbation. Because it is located in the proton transfer pathway, Lys105 also perturbs the transfer of the proton from Glu108 to RSB. The flash photolysis result corroborates the light-induced proton transport measurement. Via the comparison of the initial velocity of proton transport, we found that L105K mutants transport protons almost 6 times slower than the wild-type protein. On the basis of the flash photolysis and proton transport experiment, we developed a model that can explain the mutational effect. According to our model, the lysine group is on the proton transport pathway on the cytoplasmic side, which perturbs the donation of a proton to the retinal Schiff base from Glu108 and hence yields low proton pumping activity.

■ ASSOCIATED CONTENT

Supporting Information

Absorption spectra of the wild type and L105K at various pH values (Figure S1), absorption spectra of E108Q and L105K/E108Q at pH 7.0 (Figure S2), pH titration and absorption spectra of E108Q and L105K/E108Q at pH 5.0 and 10.0 (Figure S3), kinetics of the light-induced absorption change of E108Q and L105K/E108Q (Figure S4), global fitting parameters of the kinetics of the wild type and L105K (Table S1), and global fitting parameters of the kinetics of E108Q and L105K/E108Q (Table S2). This material is available free of charge via the Internet at http://pubs.acs.org.

■ AUTHOR INFORMATION

Corresponding Author

*Department of Frontier Materials, Nagoya Institute of Technology, Showa-ku, Nagoya 466-8555, Japan. Phone and fax: 81-52-735-5207. E-mail: kandori@nitech.ac.jp.

Funding

This work was supported by grants from the Japanese Ministry of Education, Culture, Sports, Science and Technology to H.K. (20108014 and 22247024), and K.I. (22018012).

Notes

The authors declare no competing financial interest.

■ ABBREVIATIONS

PSB, protonated Schiff base; BR, bacteriorhodopsin; PR, proteorhodopsin; DDM, dodecyl maltoside.

■ REFERENCES

(1) Kandori, H. (2006) Retinal binding proteins. In *cis-trans isomerization in biochemistry* (Dugave, C., Ed.) pp 53−75, Wiley-VCH, Freiburg, Germany.

(2) Haupts, U., Tittor, J., and Oesterhelt, D. (1999) Closing in on bacteriorhodopsin: Progress in understanding the molecule. *Annu. Rev. Biophys. Biomol. Struct. 28*, 367−399.

(3) Lanyi, J. K. (2000) Bacteriorhodopsin. *Biochim. Biophys. Acta 1460*, 1−3.

(4) Yan, B., Spudich, J. L., Mazur, P., Vunnam, S., Derguini, F., and Nakanishi, K. (1995) Spectral tuning in bacteriorhodopsin in the absence of counterion and coplanarization effects. *J. Biol. Chem. 270*, 29668−29670.

(5) Ottolenghi, M., and Sheves, M. (1989) Synthetic retinals as probes for the binding site and photoreactions in rhodopsins. *J. Membr. Biol. 112*, 193−212.

(6) Spudich, J. L., Yang, C. S., Jung, K. H., and Spudich, E. N. (2000) Retinylidene proteins: Structures and functions from archaea to humans. *Annu. Rev. Cell Dev. Biol. 16*, 365−392.

(7) Kochendoerfer, G. G., Lin, S. W., Sakmar, T. P., and Mathies, R. A. (1999) How color visual pigments are tuned. *Trends Biochem. Sci. 24*, 300−305.

(8) Sekharan, S., Sugihara, M., and Buss, V. (2007) Origin of spectral tuning in rhodopsin: It is not the binding pocket. *Angew. Chem., Int. Ed. 46*, 269−271.

(9) Coto, P. B., Strambi, A., Ferre, N., and Olivucci, M. (2006) The color of rhodopsins at the ab initio multiconfigurational perturbation theory resolution. *Proc. Natl. Acad. Sci. U.S.A. 103*, 17154−17159.

(10) Hoffmann, M., Wanko, M., Strodel, P., Konig, P. H., Frauenheim, T., Schulten, K., Thiel, W., Tajkhorshid, E., and Elstner, M. (2006) Color tuning in rhodopsins: The mechanism for the spectral shift between bacteriorhodopsin and sensory rhodopsin II. *J. Am. Chem. Soc. 128*, 10808−10818.

(11) Kakitani, T., Beppu, Y., and Yamada, A. (1999) Color tuning mechanism of human red and green visual pigments. *Photochem. Photobiol. 70*, 686−693.

(12) Mogi, T., Stern, L. J., Marti, T., Chao, B. H., and Khorana, H. G. (1988) Aspartic acid substitutions affect proton translocation by bacteriorhodopsin. *Proc. Natl. Acad. Sci. U.S.A. 85*, 4148−4152.

(13) Subramaniam, S., Greenhalgh, D. A., Rath, P., Rothschild, K. J., and Khorana, H. G. (1991) Replacement of leucine-93 by alanine or threonine slows down the decay of the N and O intermediates in the photocycle of bacteriorhodopsin: Implications for proton uptake and 13-cis-retinal−all-trans-retinal reisomerization. *Proc. Natl. Acad. Sci. U.S.A. 88*, 6873−6877.

(14) Beja, O., Spudich, E. N., Spudich, J. L., Leclerc, M., and DeLong, E. F. (2001) Proteorhodopsin phototrophy in the ocean. *Nature 411*, 786−789.

(15) Sharma, A. K., Spudich, J. L., and Doolittle, W. F. (2006) Microbial rhodopsins: Functional versatility and genetic mobility. *Trends Microbiol. 14*, 463−469.

(16) Yoshizawa, S., Kawanabe, A., Ito, H., Kandori, H., and Kogure, K. (2012) Diversity and functional analysis of proteorhodopsin in marine *Flavobacteria*. *Environ. Microbiol.*, DOI: 10.1111/j.1462-2920.2012.02702.x.

(17) Beja, O., Aravind, L., Koonin, E. V., Suzuki, M. T., Hadd, A., Nguyen, L. P., Jovanovich, S. B., Gates, C. M., Feldman, R. A., Spudich, J. L., Spudich, E. N., and DeLong, E. F. (2000) Bacterial rhodopsin: Evidence for a new type of phototrophy in the sea. *Science 289*, 1902−1906.

(18) Wang, W. W., Sineshchekov, O. A., Spudich, E. N., and Spudich, J. L. (2003) Spectroscopic and photochemical characterization of a deep ocean proteorhodopsin. *J. Biol. Chem. 278*, 33985−33991.

(19) Man, D., Wang, W., Sabehi, G., Aravind, L., Post, A. F., Massana, R., Spudich, E. N., Spudich, J. L., and Beja, O. (2003) Diversification and spectral tuning in marine proteorhodopsins. *EMBO J. 22*, 1725−1731.

(20) Friedrich, T., Geibel, S., Kalmbach, R., Chizhov, I., Ataka, K., Heberle, J., Engelhard, M., and Bamberg, E. (2002) Proteorhodopsin is a light-driven proton pump with variable vectoriality. *J. Mol. Biol. 321*, 821−838.

(21) Gomez-Consarnau, L., Gonzalez, J. M., Coll-Llado, M., Gourdon, P., Pascher, T., Neutze, R., Pedros-Alio, C., and Pinhassi, J. (2007) Light stimulates growth of proteorhodopsin-containing marine Flavobacteria. *Nature 445*, 210−213.

(22) Kralj, J. M., Spudich, E. N., Spudich, J. L., and Rothschild, K. J. (2008) Raman spectroscopy reveals direct chromophore interactions in the Leu/Gln105 spectral tuning switch of proteorhodopsins. *J. Phys. Chem. B 112*, 11770−11776.

(23) Lanyi, J. K. (2000) Molecular Mechanism of Ion Transport in Bacteriorhodopsin: Insights from Crystallographic, Spectroscopic, Kinetic, and Mutational Studies. *J. Phys. Chem. B 104*, 11441−11448.

(24) Yoshitsugu, M., Shibata, M., Ikeda, D., Furutani, Y., and Kandori, H. (2008) Color change of proteorhodopsin by a single amino acid replacement at a distant cytoplasmic loop. *Angew. Chem., Int. Ed. 47*, 3923−3926.

(25) Yoshitsugu, M., Yamada, J., and Kandori, H. (2009) Color-changing mutation in the E-F loop of proteorhodopsin. *Biochemistry 48*, 4324−4330.
(26) Krebs, R. A., Alexiev, U., Partha, R., DeVita, A. M., and Braiman, M. S. (2002) Detection of fast light-activated H^+ release and M intermediate formation from proteorhodopsin. *BMC Physiol. 2*, 5.
(27) Ikeda, D., Furutani, Y., and Kandori, H. (2007) FTIR study of the retinal Schiff base and internal water molecules of proteorhodopsin. *Biochemistry 46*, 5365−5373.
(28) Furutani, Y., Kamada, K., Sudo, Y., Shimono, K., Kamo, N., and Kandori, H. (2005) Structural changes of the complex between *pharaonis* phoborhodopsin and its cognate transducer upon formation of the M photointermediate. *Biochemistry 44*, 2909−2915.
(29) Inoue, K., Sudo, Y., Homma, M., and Kandori, H. (2011) Spectrally silent intermediates during the photochemical reactions of *Salinibacter* sensory rhodopsin I. *J. Phys. Chem. B 115*, 4500−4508.
(30) Shastri, S., Vonck, J., Pfleger, N., Haase, W., Kuehlbrandt, W., and Glaubitz, C. (2007) Proteorhodopsin: Characterization of 2D crystals by electron microscopy and solid state NMR. *Biochim. Biophys. Acta 1768*, 3012−3019.
(31) Shi, L., Ahmed, M. A., Zhang, W., Whited, G., Brown, L. S., and Ladizhansky, V. (2009) Three-dimensional solid-state NMR study of a seven-helical integral membrane proton pump: Structural insights. *J. Mol. Biol. 386*, 1078−1093.
(32) Pfleger, N., Wörner, A. C., Yang, J., Shastri, S., Hellmich, U. A., Aslimovska, L., Maier, M. S., and Glaubitz, C. (2009) Solid-state NMR and functional studies on proteorhodopsin. *Biochim. Biophys. Acta 1787*, 697−705.
(33) Hempelmann, F., Hölper, S., Verhoefen, M. K., Woerner, A. C., Köhler, T., Fiedler, S. A., Pfleger, N., Wachtveitl, J., and Glaubitz, C. (2011) His75-Asp97 cluster in green proteorhodopsin. *J. Am. Chem. Soc. 133*, 4645−4654.
(34) Ward, M. E., Shi, L., Lake, E., Krishnamurthy, S., Hutchins, H., Brown, L. S., and Ladizhansky, V. (2011) Proton-detected solid-state NMR reveals intramembrane polar networks in a seven-helical transmembrane protein proteorhodopsin. *J. Am. Chem. Soc. 133*, 17434−17443.
(35) Reckel, S., Gottstein, D., Stehle, J., Löhr, F., Verhoefen, M. K., Takeda, M., Silvers, R., Kainosho, M., Glaubitz, C., Wachtveitl, J., Bernhard, F., Schwalbe, H., Güntert, P., and Dötsch, V. (2011) Solution NMR structure of proteorhodopsin. *Angew. Chem., Int. Ed. 50*, 11942−11946.
(36) Yamada, K., Kawanabe, A., and Kandori, H. (2010) Importance of alanine at position 178 in proteorhodopsin for absorption of prevalent ambient light in the marine environment. *Biochemistry 49*, 2416−2423.
(37) Subramaniam, S., Marti, T., Rösselet, S. J., Rothschild, K. J., and Khorana, H. G. (1991) The reaction of hydroxylamine with bacteriorhodopsin studied with mutants that have altered photocycles: Selective reactivity of different photointermediates. *Proc. Natl. Acad. Sci. U.S.A. 88*, 2583−2587.